Stability assessment of roadbed affected by ground subsidence adjacent to urban railways

Ki-Young Eum[1], Young-Kon Park[2], Sang-Soo Jeon[3]

[1]Advanced infrastructure research team, Korea Railroad Research Institute, Chuldobakmulgwan-Ro 176, Uiwang City, Gyeonggi-Do 16105, South Korea

[2]Smart station research team, Korea Railroad Research Institute, Chuldobakmulgwan-Ro 176, Uiwang City, Gyeonggi-Do 16105, South Korea

[3]Department of Civil and Urban Engineering, Inje University, Inje-Ro 197, Gimhae City, Kyungsangnam-Do 50834, South Korea

Correspondence to: Sang-Soo Jeon (ssj@inje.ac.kr)

Abstract. In recent years, leakages in aged pipelines for water and sewage in urban areas have frequently induced ground loss resulting in cavities and ground subsidence causes the roadbed settlement greater than the allowable value. In this study, FLAC^{3D}, which is a three-dimensional finite-difference numerical modeling software, is used to do stability and risk level assessment for the roadbed in adjacent to urban railways with respect to various groundwater levels and the geometric characteristics of cavities. Numerical results show that roadbed settlement increases as the diameter (D) of the cavity increases and the distance (d) between the roadbed and the cavity decreases. The regression analyses results show that, as D/d is greater than 0.2 and less than 0.3, the roadbed is in the status of caution or warning. It requires a database of measurement sensors for real-time monitoring of the roadbed, structures and groundwater to prevent disasters in advance. As D/d exceeds 0.35, the roadbed settlement, which substantially increases and the roadbed is in the status of danger. Since it may result in highly probable traffic accident, train operation should be stopped and the roadbed should be reinforced or repaired. The effects of groundwater level on the roadbed settlement are examined and the analyses results indicate that a roadbed settlement is highly influenced by groundwater levels to an extent greater than even the influence of the size of the cavity.

1 Introduction

Urban railways in South Korea have been initiated from the Seoul subway 1st line in1974 and have been operating in Seoul city and several metropolitan cities. The number of passengers using urban railway are being increased and it has played a significantly important role in public transportation for urban development. Urban railway is defined as transportation facility and method for smooth transportation in the city and includes light rail transit and subway as indicated in the law of urban railway (Ministry of land, 2017).

Risk management associated with safety is a fundamental focus in railway operations. It has been integrated into global safety management system of railways (Berrado et al., 2010) and developed to allow a rapid risk assessment using a common risk score matrix (Braband, 2011). As roadbed settlements exceed the allowable limits, it may result in track irregularity and derailments of trains causing heavy loss of life. Therefore, risk management tools are developed to deal with track safety by controlling and reducing the risk of derailments (Zarembski et al., 2006). In this study, methods to secure the stability of roadbeds have been examined using numerical analysis.

Numerical analyses have been widely used for risk assessment. Numerical analyses using three-dimensional geotechnical codes were carried out to predict the subsidence area and its interaction with buildings (Castellanza et al., 2015) and a three-dimensional groundwater flow model for risk evaluation was developed to be an effective management strategy (Ashfaque et al., 2017). The coupling of numerical models and monitoring data contribute to undertake efficient risk reduction policies (Bozzano et al., 2013). Especially using FLAC, which is a finite-difference numerical code especially specialized in the area of geotechnical engineering, numerical computations to simulate the influence of rainfall (Pisani, 2010), both acoustic emission (AE) activities at AE sensor locations of

the Kannagawa cavern (Cai et al., 2007), and a comprehensive pump test at Sellafield (Hakami, 2001) showed good agreement with field monitoring results. In this study, FLAC^{3D}, which is a three-dimensional finite-difference numerical code especially specialized in the area of geotechnical engineering, is adopted for numerical analysis.

Research on stability assessment and reinforcement of railway roadbeds has been actively carried out, but the effect of the cavity adjacent to urban railways on roadbed behavior has rarely studied. In recent years, the number of accidents induced by cavities larger than 2 m in diameter has increased especially in highly populated cities in South Korea. Therefore, the residents in these cities were terrified of cavities after the accidents (Shin and Roh, 2006). Especially, ground subsidence near subways due to self-weight and/or surcharge loading was around 60% (Lee and Kang, 2014). Changes in groundwater levels may cause increased occurrences of ground subsidence because the lowering of groundwater levels lead to ground settlement (Lee et al., 2015). Groundwater level influences both ground settlement and stability of underground structures. Deep excavation of the ground adjacent to urban railways has a significance influence on the allowable tensile strength of underground structures (Lee at al., 2017). If large underground cavities are located at nearby roadbeds, there is a high potential of ground subsidence.

Ground subsidence (Fig. 1) in South Korea occurred at nearby urban railways most recently (Kyunghang times, 2016). The ground subsidence (Fig. 1a) occurred with a cavity of depth 5 m, width 8 m, and length 80 m near the Seokchon subway station in Seoul City. The accident was induced by the inappropriate deep excavation near the subway. The ground subsidence (Fig. 1b) was caused by the leakage of a water pipeline with a large-scale cavity of depth 21 m, width 11 m, and length 12 m near Bakchon subway station in Incheon City (Newshankuk, 2016). The ground subsidence (Fig. 1c) occurred near Samseongjungang subway station. Six cavities were found almost simultaneously in Seoul City (Kyunghang times, 2016). A small-scale cavity of depth 2.2 m (Fig. 1d) occurred near Janghanpyeong subway station in Seoul City, but the cause of this accident has not been clarified. The accident was assumed to be caused by inappropriate recovery construction near subway extension.

Ground subsidence with a cavity having depth 3.6 m (Fig. 1e) occurred as the replacement work of a sewage pipeline was carried out at Texas in the US (Wikitree, 2016). Ground subsidence with a cavity having a width of 15 m (Fig. 1f) occurred as tunnel excavation work for subway extension was carried out at Fukuoka in Japan (Chosun Ilbo, 2016). Ground subsidence with a cavity of width 25 m (Fig. 1g) occurred as a 50 m tunnel excavation near the light rail transit was carried out at Ottawa in Canada (Yonhap news, 2016). Ground subsidence with a cavity of depth 10 m (Fig. 2h) occurred as subway construction was carried out near Guangzhou in China (Sisa china, 2016). Ground subsidence with a large-scale cavity in urban areas is highly correlated with the undiscerned development of urban areas, abuse of groundwater and inappropriate underground construction.

Figure 1. Ground subsidence nearby subway of urban railway: **(a)** Seokchon subway station, **(b)** Bakchon subway station, **(c)** Samseongjungang subway station, **(d)** Janghanpyeong subway station in South Korea, **(e)** Texas in the US, **(f)** Fukuoka in Japan, **(g)** Ottawa in Canada, and **(h)** Guangzhou in China.

80% of the ground subsidence occurred from 2010 until the beginning of 2014 in Seoul City was induced by aged pipelines for water and sewage (Oh et al., 2015). Since 48% and 30% of sewage pipelines in Seoul city were constructed more than thirty and fifty years ago, respectively. Aged pipelines for water and sewage pipelines cause

numerous cavities in the near future (The Segye times, 2016).

As a cavity exists at the center of the railway track in the box structures of urban railways, its influence on box structures and roadbed settlements has been examined to observe the effects of cavities adjacent to the roadbeds of urban railways (Lee at al., 2015). A method to establish a database was proposed to prevent and manage the disasters (Choi et al., 2007).

As a cavity exists adjacent to the roadbed, in this study, a three-dimensional numerical analysis using FLAC^{3D} is carried out to assess both roadbed stability and risk level with respect to the distance between the center of the roadbed and the center of the cavity, diameter of the cavity, and groundwater levels.

2 Numerical analysis

In the following sections, the FLAC^{3D} given in this work are briefly described in the following sections by paraphrasing from those of Itasca Consulting Group (2002).

2.1 Theoretical background of FLAC^{3D}

FLAC^{3D} (Fast Lagrangian Analysis of Continua in three Dimensions) is numerical modeling software for advanced geotechnical analysis of soil, rock, groundwater, and ground support in three dimensions. FLAC is used for analysis, testing, and design by geotechnical, civil, and mining engineers (Itasca Consulting Group Inc., 2002). It is designed to accommodate any kind of geotechnical engineering project that requires continuum analysis.

The mechanics of the medium are derived from general principles (definition of strain, laws of motion), and the use of constitutive equations defining the idealized material. The resulting mathematical expression is a set of partial differential equations, relating mechanical (stress) and kinematic (strain rate, velocity) variables, which are to be solved for particular geometries and properties, given specific boundary and initial conditions.

An important aspect of the model is the inclusion of the equations of motion, although FLAC3D is primarily concerned with the state of stress and deformation of the medium near the state of equilibrium. It will be shown, in the numerical implementation section, that the inertial terms are used as means to reach, in a numerically stable manner, the equilibrium state.

2.1.1 Conventions

In the Lagrangian formulation adopted in FLAC^{3D}, a point in the medium is characterized by the vector components x_i, u_i, v_i and d_{vi}/d_t, i=1,3 of position, displacement, velocity and acceleration, respectively. As a notation convention, a bold letter designates a vector or tensor, depending on the context. The symbol a_i denotes component i of the vector $[a]$ in a Cartesian system of reference axes; A_{ij} is component (i, j) of tensor $[A]$. Also, a, i is the partial derivative of a with respect to x_i. (α can be a scalar variable, a vector or tensor component.) By definition, tension and extension are positive. The Einstein summation convention applies, but only on indices i, j and k, which take the values 1, 2, 3.

2.1.2 Stress

The state of stress at a given point of the medium is characterized by the symmetric stress tensor σ_{ij}. The traction vector $[t]$ on a face with unit normal $[n]$ is given by Cauchy's formulae (tension positive):

$$t_i = \sigma_{ij} \tag{1}$$

2.1.3 Rate of Strain and Rate of Rotation

Let the particles of the medium move with velocity $[v]$. In an infinitesimal time dt, the medium experiences an infinitesimal strain determined by the translations $v_i dt$, and the corresponding components of the strain-rate tensor may be written as

$$\xi_{ij} = 1/2(v_{i,j} + v_{j,i}) \quad (2)$$

where partial derivatives are taken with respect to components of the current position vector $[x]$. For later reference, the first invariant of the strain-rate tensor gives a measure of the rate of dilation of an elementary volume. Aside from the rate of deformation characterized by the tensor ξ_{ij}, a volume element experiences an instantaneous rigid-body displacement, determined by the translation velocity $[v]$, and a rotation with angular velocity,

$$\Omega_i = -1/2 e_{ijk}\omega_{jk} \quad (3)$$

where e_{ij} is the permutation symbol, and [ω] is the rate of rotation tensor whose components are defined as

$$\omega_{ij} = 1/2(v_{i,j} + v_{j,i}) \quad (4)$$

2.1.4 Equations of Motion and Equilibrium

Application of the continuum form of the momentum principle yields Cauchy's equations of motion:

$$\sigma_{ij,j} + \rho b_i = \rho(d_{vi}/d_t) \quad (5)$$

where ρ is the mass per unit volume of the medium, $[b]$ is the body force per unit mass, and $d[v]/dt$ is the material derivative of the velocity. These laws govern, in the mathematical model, the motion of an elementary volume of the medium from the forces applied to it. Note that in the case of static equilibrium of the medium, the acceleration $d[v]/dt$ is zero, and Eq. (5) reduces to the partial differential equations of equilibrium:

$$\sigma_{ij,j} + \rho b_i = 0 \quad (6)$$

2.1.5 Boundary and Initial Conditions

The boundary conditions consist of imposed boundary tractions (see Eq. (1)) and/or velocities (to induce given displacements). In addition, body forces may be present. Also, the initial stress state of the body needs to be specified.

2.1.6 Constitutive Equations

The equations of motion Eq. (5), together with the definitions Eq. (2) of the rates of strain, constitute nine equations for fifteen unknowns — the unknowns being the 6 + 6 components of the stress- and strain-rate tensors and the three components of the velocity vector. Six additional relations are provided by the constitutive equations that define the nature of the particular material under consideration. They are usually given in the form

$$[\dot{\sigma}]_{ij} = H_{ij}(\sigma_{ij}, \xi_{ij}, k) \quad (7)$$

in which $[\dot{\sigma}_{ij}]$ is the co-rotational stress-rate tensor, [H] is a given function, and k is a parameter that takes into account the history of loading. The co-rotational stress rate $[\dot{\sigma}]$ is equal to the material derivative of the stress as it would appear to an observer in a frame of reference attached to the material point and rotating with it at an angular velocity equal to the instantaneous value of the angular velocity [Ω] of the material. Its components are defined as

$$[\dot{\sigma}]_{ij} = (d\sigma_{ij}/d_t) - \omega_{ik}\sigma_{kj} + \sigma_{ik}\omega_{kj} \quad (8)$$

in which d[σ]/dt is the material time derivative of [σ], and [ω] is the rate of rotation tensor.

2.2 Conditions for numerical analysis

The Mohr-Coulomb failure model has been used for the analysis (Itasca Consulting Group Inc., 2015). Since there

are various causes and sizes of the cavity of ground subsidence occurring near urban railway, it is very difficult to simulate the process of cavity generation. A circular cavity below the ground surface has been modeled with respect to diameters (D) of 4-10 m, which is selected by historical events as described in previous section. Distances of 15-25 m from the cavity to the center of the roadbed and various groundwater levels are arbitrarily selected for roadbed settlement influenced by given size of cavity. The analysis is performed based on the configuration of the analysis (Fig. 2). As shown in the figure, roller supports prevent normal translations, but capable of tangential translations and/or rotations. There is a single linear reaction force in either vertical or horizontal directions.

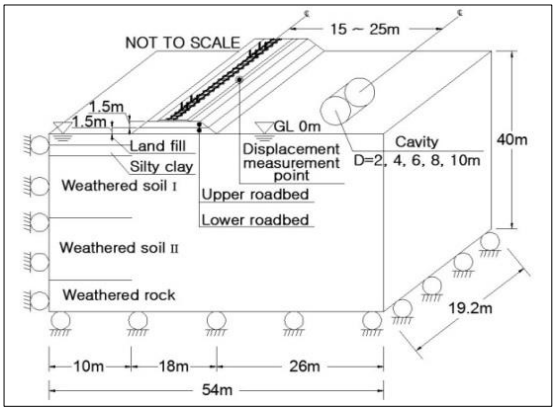

Figure 2. Configuration of the railway roadbed and cavity

2.2.1 Ground conditions

An embankment consists of the lower roadbed, upper roadbed, and gravel ballast. The roadbed width at the bottom of the ballast is 8m. The widths of its bottom and top are 5.1 m and 3.3 m, respectively, and its slope is 1:1.8. In-situ soil consists of reclaimed soil, silty clay, weathered soil, and weathered rock. Its physical properties listed in Table 1 are obtained from lab experiments of soil sampled at a construction site.

2.2.2 Physical properties of rail, rail pad, and prestressed concrete (PC) sleeper

KS60 rail and prestressed concrete (PC) sleeper commonly used in gravel ballast have been used for the numerical analysis. A rail pad, which is widely used to minimize vibration and impact loading during train operation is made of ethylene vinyl acetate (EVA). However, in this study, a thermoplastic polyurethane (TPU) rail pad, which is more economical and has higher tensile strength has been used for the numerical analysis. Its properties are listed in Table 1. The beam element is used for the rail and rail pad.

2.2.3 Applied train loading

An axial load of the urban railway train (16 tons) is applied for the numerical analysis. The effective loading is estimated by multiplying 1.2 with half of the axial load considering a wheel loading increment of 20% and a marginal safety of deficiency of the cant. Dynamic loading to reflect dynamic impact ratio (Fig. 3) was estimated by multiplying 1.2 with the effective loading (Ministry of land, 2013).

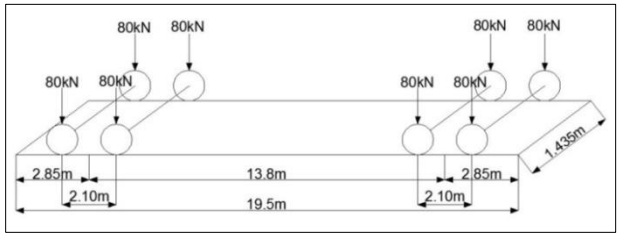

Figure 3. Configuration of the train load

Table 1. Physical properties of soil, rail, PC sleeper and the rail pad

	Soil type	Height (m)	Unit weight (kN/m^3)	Elastic modulus (kPa)	Poisson's ratio (υ)	Cohesion (kPa)	Friction angle (°)	Coefficient of permeability (cm/s)	K_o
Soil	Ballast stone	0.3	19.0	133,900	0.30	-	35	-	0.43
	Upper roadbed	1.5	18.0	81,600	0.20	3.0	32	-	0.47
	Lower roadbed	1.5	18.0	51,000	0.30	10.0	30	-	0.50
	Land fill	1.5	17.0	30,000	0.35	5.0	24	1.0×10^{-3}	0.59
	Silty clay	1.5	17.0	20,000	0.35	5.0	25	5.0×10^{-4}	0.58
	Weathered soil Ⅰ	15.0	19.0	75,000	0.33	10.0	30	1.0×10^{-4}	0.50
	Weathered soil Ⅱ	15.0	19.0	70,000	0.33	10.0	33	1.0×10^{-4}	0.46
	Weathered rock	7.0	20.0	110,000	0.31	60.0	42	1.0×10^{-5}	0.33

KS60 rail	Area (mm^2)	Unit weight (kN/m^3)	Elastic modulus (kPa)	Moment of inertia(m^4)	
				I_{XX}	I_{YY}
	7,741	77.5	$21,000\times10^4$	$30,820\times10^{-9}$	$5,120\times10^{-9}$

PC sleeper	Length (m)	Width (m)	Height (m)	Interval between sleepers (m)
	2.45	0.28	0.20	0.58

Rail pad	Thickness (mm)	Unit weight (kN/m^3)	Vertical spring coefficient of rail pad (kPa)
	5	11.5	15.3×10^7

2.3 Allowable settlement of the roadbed

In general, an allowable settlement of 10 mm has been recommended in South Korea. The vibratory loading induces the gravel to be in a loose state, and frequent repairs of ballasts are required. Therefore, an allowable settlement of 2.5 mm is used to attain additional marginal safety considering the compressive displacement of both the rail pad and ballasts, settlement of rail, ride quality, and both water inflow and cracks in the pavement surface of roadbeds (Jeon, 2014).

3 Roadbed Settlement and Stability

3.1 Roadbed settlement

The contours of ground settlement are presented for how the roadbed (Fig. 4) is influenced by a cavity adjacent to the urban railways. The contours of ground settlement are presented for cavities with diameters of 8 m and 10 m, respectively, at a distance of 20 m between the center of the roadbed and the center of the cavity. As shown in the figures, ground settlement increases as the diameter of the cavity increases. As a cavity is generated on the right side of the roadbed, the right end of the roadbed is significantly settled down.

(a)

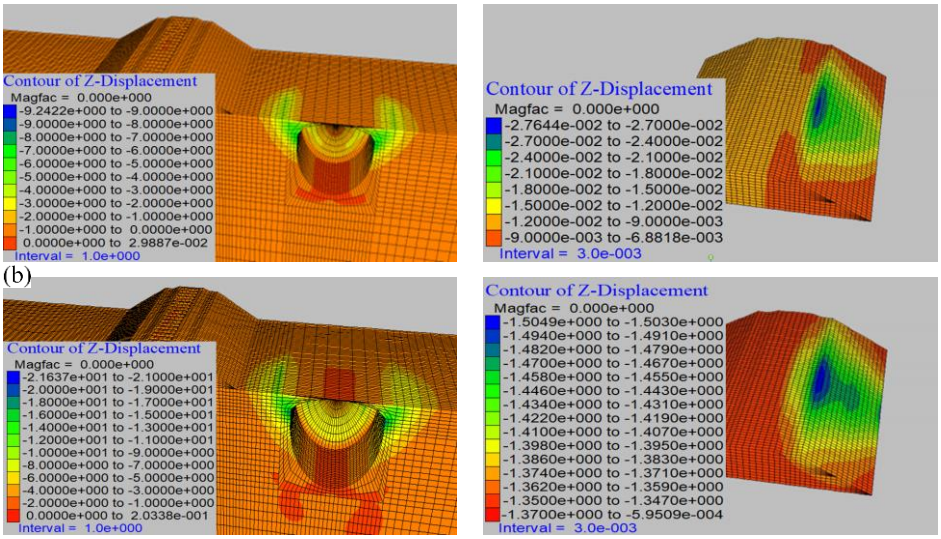

Figure 4. Vertical displacement contour of the roadbed at a distance of 20 m between the center of roadbed to the center of the cavity=20 m with respect to diameter of the cavity: **(a)** Diameter = 8 m and **(b)** Diameter = 10 m.

The analysis results (Fig. 5) are presented for cavities with diameters of 4-10 m. As the variation from 15 to 20 m in the distances between the center of the roadbed and the center of the cavity is applied to the 10 m cavity, roadbed settlements are calculated with respect to various diameters of the cavity. The cavity with a diameter of 10 m at a distance of 20 m has little influenced on the roadbed. However, as the diameter of the cavity at the same distance exceeds 10 m, the roadbed settlement exceeds the allowable value. As cavities with diameters of 8 and 6 m are generated, at distances less than 18 and 15 m, it exceeds the allowable settlement and may result in an accident.

The risk level has been estimated by the occurrence of roadbed settlements. Its risk level has been defined by the value of the roadbed settlements relative to the allowable settlement. The risk level is defined as safe (not problematic for both ride quality and track repair), caution (not problematic for track repair), warning (between caution and danger), and danger (highly probable traffic accident) as a settlement is equal to or less than 2.5 mm, greater than 2.5 mm and equal to or less than 4 mm, greater than 4 mm and equal to or less than 9mm, and greater than 9 mm, respectively.

Roadbed settlement increases as the diameter (D) of the cavity increases and the distance (d) between the roadbed and the cavity decreases. Therefore, in this study, the roadbed settlement is examined with respect to D normalized by d (Fig. 6). The regression analyses results show medium to high correlations of r^2=0.72. As D/d is greater than 0.2 and less than 0.3, the roadbed settlement is approximately 5 mm. It requires that a database of measurement sensors should be established for real-time monitoring of the roadbed, structures and groundwater to prevent disasters in advance. As D/d exceeds 0.35, the roadbed settlement substantially increases and is greater than 10 mm. Since it may result in highly probable traffic accident, train operation should be stopped and the roadbed should be reinforced or repaired.

3.2 Effects of groundwater level

In this study, the effects of groundwater level on the roadbed settlement are examined and it is lowered until the allowable settlement value of the roadbed is satisfied. The maximum distance between the roadbed and the cavity for the analysis is determined as the maximum value for the satisfied allowable settlement with no groundwater condition. A stability assessment of the roadbed has been carried out at the distance of 20 m for both 4 and 6 m diameter cavities and at 25 m for both the 8 and 10 m diameter cavities.

The contours of ground settlement (Fig. 7) are presented to examine the groundwater level (GWL) effects in the case of the 8 m diameter cavity located at a distance of 25 m from the roadbed to cavity. The contours of ground settlement are presented with GWL on the ground surface and 20 m below it, respectively (Figs. 7a and 7b). The settlement of the roadbed is highly subject to groundwater levels.

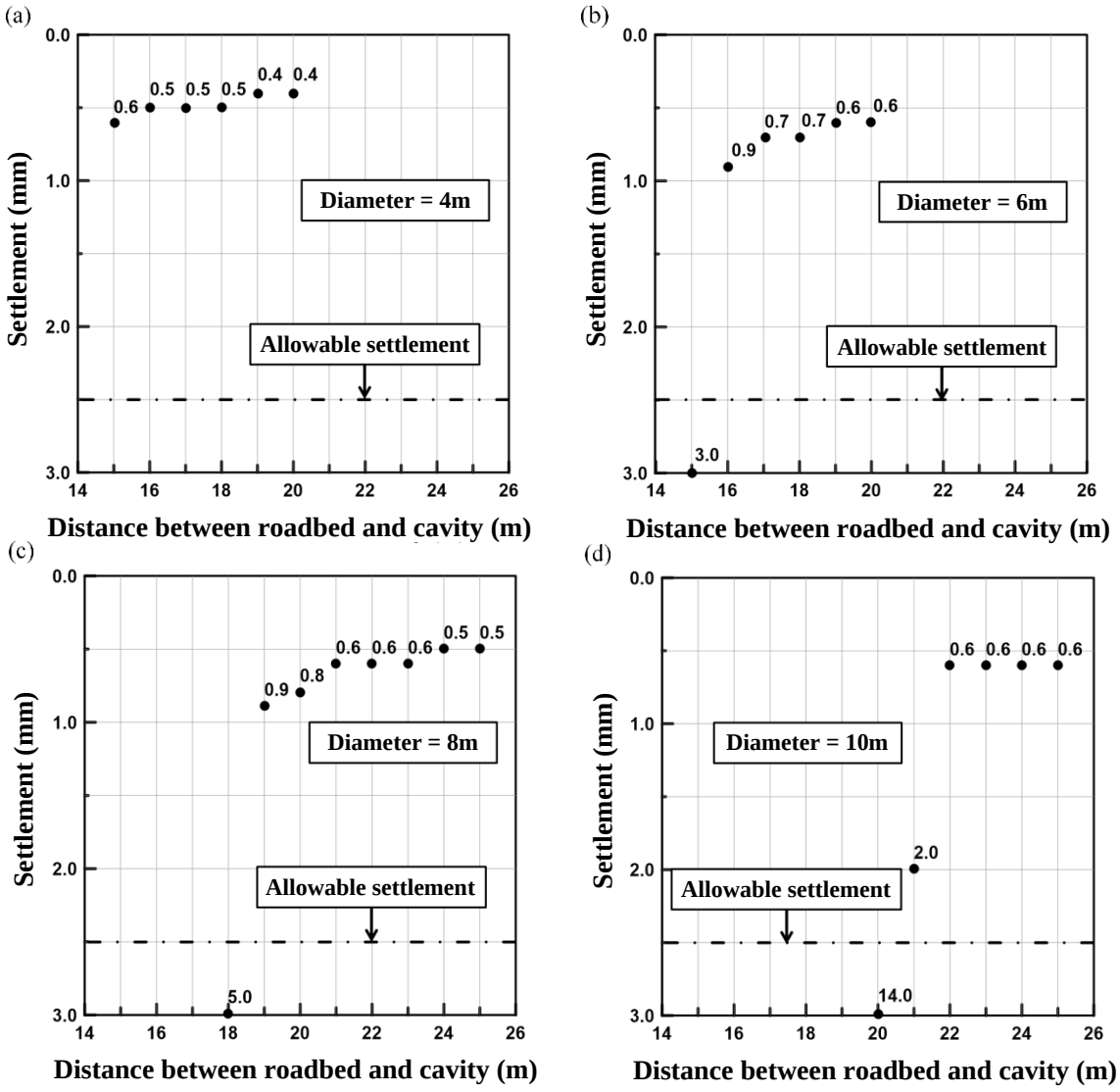

Figure 5. Roadbed settlement with respect to distance between roadbed and cavity: **(a)** Diameter = 4 m, **(b)** Diameter = 6 m, **(c)** Diameter = 8 m, and **(d)** Diameter = 10 m.

The roadbed settlement (Fig. 8) is highly influenced by groundwater. Ground settlement for 4 and 6 m diameter cavities located at a distance of 20 m from the roadbed (Figs. 8a and 8b) satisfies the allowable value for GWL = (-) 4 and (-) 12m, respectively. The ground settlement for 8 and 10 m diameter cavities located at a distance of 25 m from the center of the roadbed (Figs. 8c and 8d) has substantially decreased as groundwater level is 8 and 15 m below the ground surface, respectively, and satisfies the allowable value as its level is 18 and 22 m below the ground surface, respectively. It indicates that a roadbed settlement is highly influenced by groundwater levels to an extent greater than even the influence of the size of the cavity.

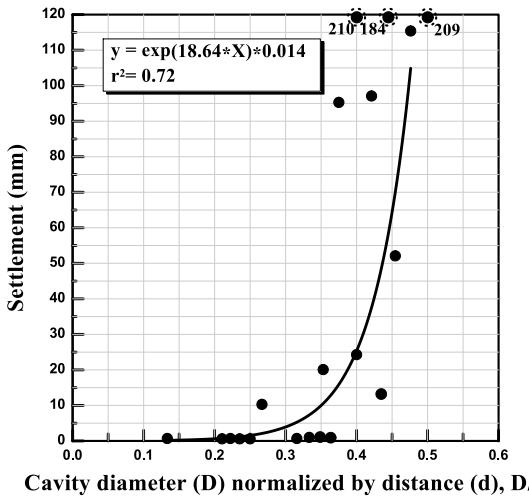

Figure 6. Regression analysis of roadbed settlements with respect to the diameter of the cavity and distance between roadbed and the cavity

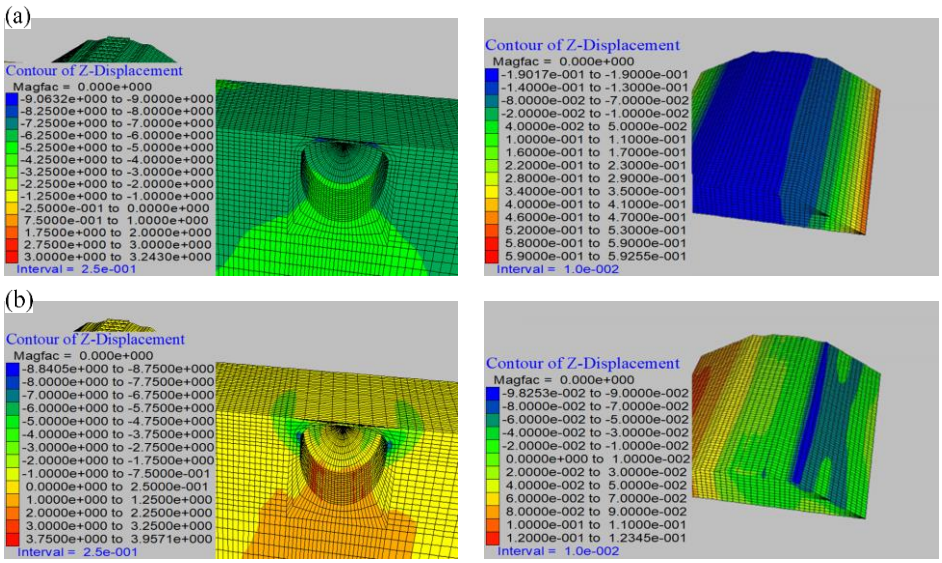

Figure 7. Vertical displacement contours of the roadbed for a cavity diameter 8 m, at the roadbed-to-cavity distance of 25 m: **(a)** GWL = ground surface and **(b)** GWL = (-) 8 m.

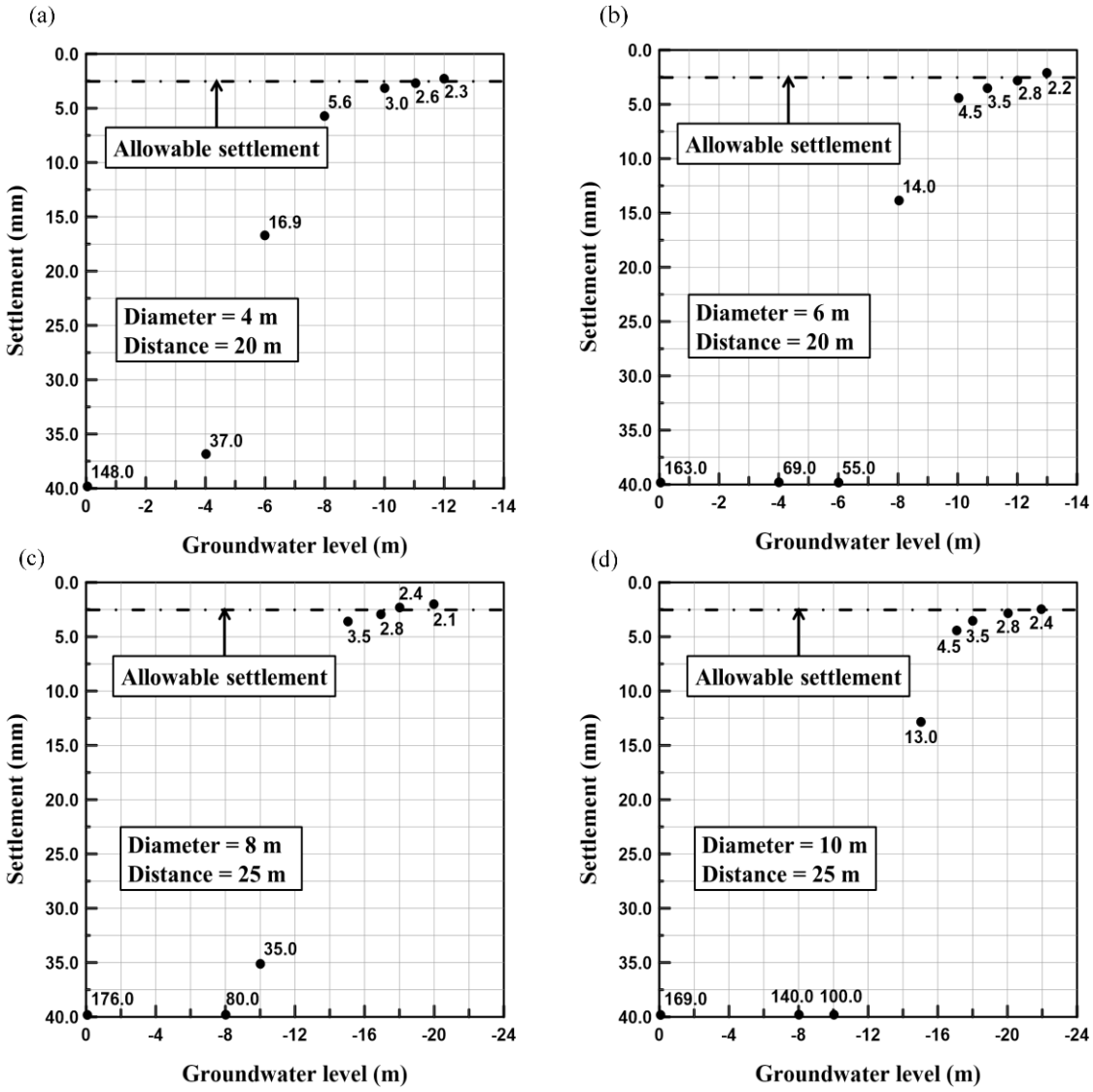

Figure 8. Roadbed settlement with respect to the groundwater level: **(a)** Diameter of the cavity = 4 m and distance of roadbed from the center of the cavity = 20 m, **(b)** Diameter of the cavity = 6 m and distance of the roadbed from the center of cavity =20 m, **(c)** Diameter of the cavity = 8 m and distance of the roadbed from the center of cavity = 25 m, and **(d)** Diameter of the cavity = 10 m and the distance of the roadbed from the center of the cavity = 25 m.

Table 2. Risk level of the roadbed with respect to the diameter of the cavity and the distance between the roadbed to the cavity for the groundwater condition

(Computation time: 3 weeks)

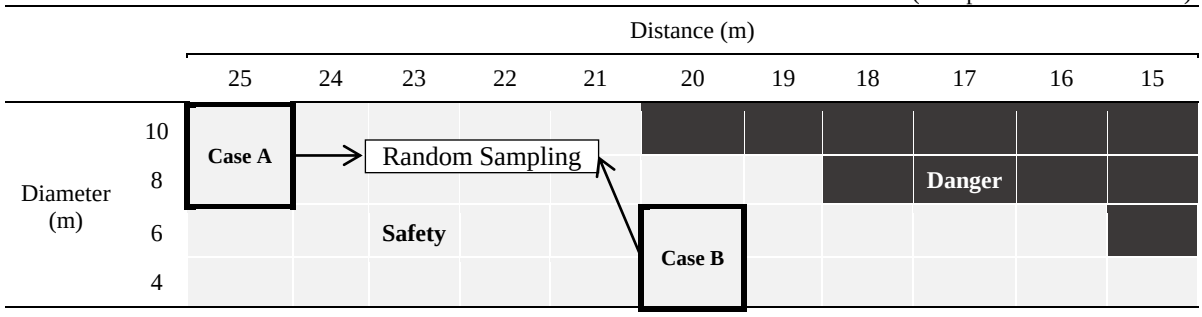

(Computation time: 4 days)

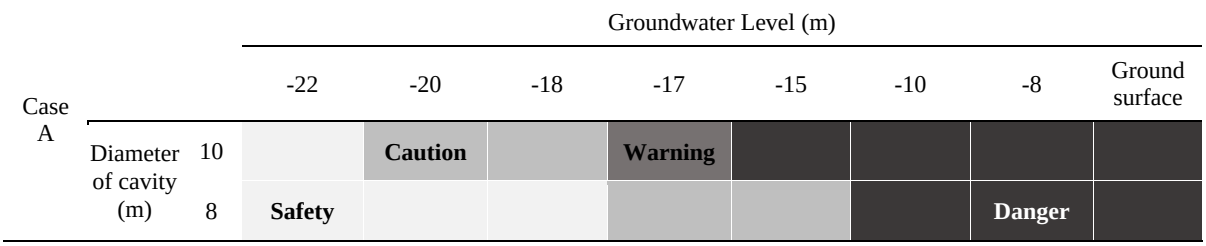

(Computation time: 3 days)

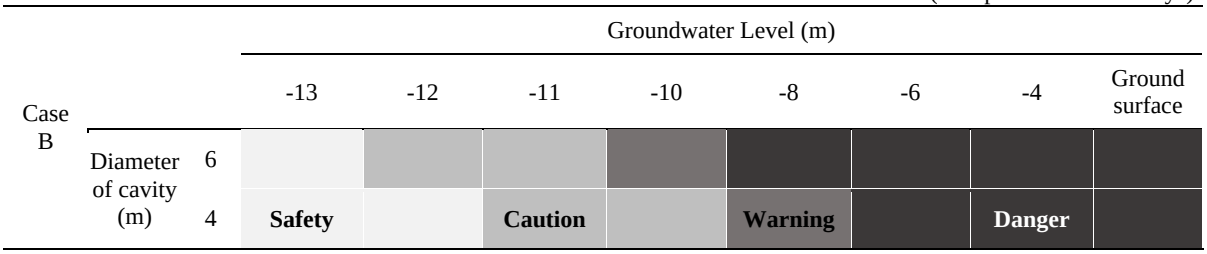

※ Safety(Settlement≤2.5mm), Caution(2.5mm<Settlement≤4.0mm), Warning(4.0mm<Settlement≤9.0mm), Danger(9.0mm<Settlement)

4 Conclusions

The number of occurrences of ground subsidence induced by a leakage of aged pipelines for water and sewage in urban areas resulting in various sizes of cavity near the urban railway in Seoul City has been found to increase and it may cause the roadbed settlement to exceed the allowable value. A large-scale cavity is rarely found, but if it is close to the roadbed, the roadbed is highly influenced by the cavity and may cause train derailment.

In this study, numerical analyses are carried out to estimate roadbed stability and its risk level associated with various groundwater levels, sizes of cavities. The analyses results show that roadbed settlement increases as the diameter (D) of the cavity increases and the distance (d) between the roadbed and the cavity decreases. The regression analyses results show that, as D/d is greater than 0.2 and less than 0.3, a database of measurement sensors should be established for real-time monitoring of the roadbed, structures and groundwater to prevent disasters in advance. As D/d exceeds 0.35, the roadbed settlement, which substantially increases and is in the status of danger, may result in highly probable traffic accident. Therefore, train operation should be stopped and the roadbed should be reinforced or repaired. The effects of groundwater level on the roadbed settlement are examined at the distance of 20 m for both 4 and 6 m diameter cavities and at 25 m for both 8 and 10 m diameter cavities. Ground settlement for 4 and 6 m diameter cavities located at a distance of 20 m from the roadbed satisfies the allowable value for GWL = (-) 4 and (-) 12m, respectively. The ground settlement for 8 and 10 m diameter cavities located at a distance of 25 m from the center of the roadbed has substantially decreased as GWL is 8 and 15 m below the ground surface, respectively, and satisfies the allowable value as its level is 18 and 22 m below the ground surface, respectively. It indicates that a roadbed settlement is highly influenced by groundwater levels to an extent greater than even the influence of the size of the cavity.

Acknowledgements. This work was supported by the 2017 INJE University research grant.

References

Ashfaque, K., Kladias, M., Sager, S., and Schlekat, T.: Numerical modeling to evaluate hydrological dynamics and risk assessment of bottom ash ponds at a former coal-fired electric power plant, World of coal ash conference, 1-13, 2017

Berrado, A., El-Loursi, E., Cherkaoui, A., and Khaddour, M.: A Framework for Risk Management in Railway Sector: Application to Road-Rail Level Crossings. Open transportation Journal, Bentham Open, 19p., 2010.

Braband, J.: Rapid Risk Assessment of Technical Systems in Railway Automation, Proc. Of the Australian System Safety Conference, 21 -26, 2011.

Bozzano, F., Cipriani, I., Esposito, C., Martino, S., Mazzanti, P., Prestininzi, A., Rocca, A., and Mugnozza, G. S.: Landslide risk reduction by coupling monitoring and numerical modeling, International conference Vajont 1963-2013. Thoughts and analyses after 50 years since the catastrophic landslide, 315-322, 2013

Cai, M., Kaiser, P. K., Morioka H., Minami, M., Maejima, T., Tasaka, Y., and Kurose, H.: FLAC/PFC coupled numerical simulation of AE in large-scale underground excavations, International Journal of Rock Mechanics & Mining Sciences, 44, 550-564, 2007.

Castellanza, R., Orlandi, G. M., Prisco, C. di, Frigerio, G., Flessati, L., Fernandez Merodo J. A., Agliardi, F., Grisi, S., and Crosta, G. B.: 3D numerical analyses for the quantitative risk assessment of subsidence and water flood due to the partial collapse of an abandoned gypsum mine. IOP Conf. Series: Earth and Environmental Science, 26, 1-7, 2015.

Choi, C. Y., Kim, D. S., Lee, J. W., and Shin, M. H.: Development of Database System for Management of Roadbed Settlement in High Speed Railway, Proceedings of Korean Society for Railway Fall Conference, 496-500, 2007.

Chosunilbo: Excavations for 15-m diameter large-scale sinkhole Fukuoka in Japan, http://news.chosun.com/site/data/html dir/2016/11/08/2016110801318.html, last access: December 2016.

Hakami, H: Rock Characterisation facility (RCF) shaft sinking – numerical computations using FLAC, International Journal of Rock Mechanics & Mining Sciences, 38, 59-65, 2001.

Itasca Consulting Group, Inc: Outline of FLAC3D, https://www.itascacg.com/software/flac3d#slideshow-6, last access: June 2017.

Itasca Consulting Group, Inc: FLAC3D Manual-Theory and Background, Minnesota, USA, 2002.

Jeon, S.-S.: Roadbed behavior subjected to tilting-train loading at rail joint and continuous welded rail, Journal of Central South University, 21, 2962-2969, 2014.

Kyunghang times: Additional finings of ground subsidence in Seckchon subway in Seoul, http://news.khan.co.kr/kh_news/khan_art_view.html?artid=201408211343301&code=940100, last access: December 2016.

Kyunghang times: '6; sinkholes concurrence at the same time' nearby Sanseongjungang of subway 9th line station, http://sports.khan.co.kr/culture/sk_index.html?cat=view&art_id=201504031002483&sec_id=562901&pt=nv, last access: December 2016.

Lee, H. J., Lee, Y. T., Choi, I. W., Lee, M. S., and Lee, T. G.: Investigation of Settlement of Concrete Track on High-Speed Railway Due to Groundwater Variation, Journal of the Korean Society for Railway, 20, 248-256, 2017.

Lee, J. H., Lee, H. S., and Lee, I. H.: IoT-based Convergence Technology for Urban Underground Sinkhole Prediction, in: 2015 Summer meeting of The institute of electronics and information engineering, The institute of electronics and information engineering, 1735-1737, 2015.

Lee, K. Y. and Kang, S. J.: Causes and Countermeasures of Sinkhole Swallowed the City, Issue and Analysis, 156, 1-23, 2014.

Lee, S. J., Lee, J. W., Jung, Y. N., and Cho, H. J.: Sensitivity Analysis of the Deformations caused by Cavity Generation in Subway Trackbed Foundation using the FEA, Proceedings of Korean Society for Railway Fall Conference, Yeosu, 1480-1485, 2015.

Ministry of Land, Infrastructure and Transport, Seoul, Korea, available at: http://www.molit.go.kr/portal.do, last access: 15 June 2015.

Ministry of Land, Infrastructure and Transport.: Seoul, Korea, available at: http://www.molit.go.kr/portal.do, last access: 15 May 2017.

Newshankuk: Asphalt road in swallowed by sinkhole brief moment, http://www.newshankuk.com/news/content.asp?fs=12&ss=57&news_idx=20120220170708129 1, last access: December 2016.

Oh, D. W., Kong, S. M., Lee, D. Y., Yoo, Y. S., and Lee, Y. J.: Effects of Reinforced Pseudo-Plastic Backfill on the Behavior of Ground around Cavity Developed due to Sewer Leakage, Journal of the Korean Geoenvironmental Society, 16, 13-22, 2015.

Pisani, G., Castelli, M., and Scavia, C.: Hydrogeological model and hydraulic behavior of a large landslide in the Italian Western Alps. Nat. Hazards Earth Syst. Sci., 10, 2391-2406, 2010.

Segye Ilbo: Half of sewage pipelines left for thirty years without maintenance leads to disaster of sinkhole, http://www.segye.com/newsView/20150322002265, last access: 3 December 2016.

Shin, E. C. and Roh, J. M.: Estimation of RPS Method Using 3-Dimensional Numerical Analysis, Journal of the Korean Society

435 for Railway, 9, 174-179, 2006.
436 Sisa China: Three of buildings one subsidence at Guangzhou in China, http://sscn.kr/news/view.html?section=1&
437 category=5&no=3561, last access: December 2016.
438 Wikitree: “Giant sinkhole” resulting in rushed car and depth of sheriff, http://www.wikitree.co.kr/main/news_view.
439 php?id=284413, last access: December 2016.
440 Yonhap news: Large-scale at Ottawa in Canada sinkhole, http://www.yonhapnews.co.kr/bulletin/2016/06/09/0200000000
441 AKR20160609069000009.HTML, last access: December 2016.
442 Zarembski, A. M. and Palese, J. W.: Managing Risk on the Railway Infrastructure, 7th World Congress on Railway Research, 1-
443 7, 2006